

Properties of a new magnetic material: $\text{Sr}_2\text{FeMoO}_6$

D D SARMA^{†*} and SUGATA RAY

Solid State and Structural Chemistry Unit, Indian Institute of Science,
Bangalore 560 012, India

[†]Also at Jawaharlal Nehru Centre for Advanced Scientific Research,
Bangalore, India

e-mail: sarma@sscu.iisc.ernet.in

Abstract. Recently, there have been a large number of investigations of the physical properties of $\text{Sr}_2\text{FeMoO}_6$ and related compounds, in view of their significant negative magnetoresistive property at room temperature and in low applied magnetic fields. We review these investigations, detailing the microscopic mechanism controlling the electronic and magnetic properties of this system.

Keywords. Room temperature colossal magnetoresistance; order–disorder effects; electronic and magnetic structures.

1. Introduction

Following the discovery¹ of the spectacular decrease in electrical resistivity on application of a magnetic field, known as Colossal Magnetoresistance (CMR), there has been tremendous increase in research activities on doped perovskite manganites. The interest in these compounds stems both from the fundamental issues involved and the technological implications in terms of magnetic storage devices. The basic properties of the manganites are now well-understood in terms of the strong coupling of electronic, magnetic and structural degrees of freedom². However, technological exploitation of the CMR property of manganites is primarily limited by the requirements of low temperature and high applied magnetic field for obtaining appreciable negative magnetoresistance effect in these compounds. Recently, a double perovskite oxide, $\text{Sr}_2\text{FeMoO}_6$, has been reported to exhibit an appreciable negative CMR even at room temperature and low magnetic fields³. The reason for this improved MR property in this compound at a relatively higher temperature arises primarily from the fact that $\text{Sr}_2\text{FeMoO}_6$ has a surprisingly high magnetic ordering temperature ($\sim 415\text{ K}$)⁴ compared to manganites, since the largest MR response is expected close to the magnetic T_C . There are also some fundamental aspects which distinguishes $\text{Sr}_2\text{FeMoO}_6$ from the group of perovskite manganites. The most important differences are (i) the CMR property is present in the *undoped* parent compound, $\text{Sr}_2\text{FeMoO}_6$, unlike manganites, (ii) electron–phonon coupling does not appear to be crucial for the observed properties of this compound, and finally (iii) the conventional double exchange mechanism⁵, universally accepted in the case of doped manganites, is absent in $\text{Sr}_2\text{FeMoO}_6$ ⁶. Despite the apparent simplicity of this system, several important controversies exist concerning the details of the electronic and magnetic structures of

*For correspondence

this compound. For example, the formal oxidation states of Fe and Mo ions in $\text{Sr}_2\text{FeMoO}_6$ have been debated in the recent literature. In some early reports⁷, it has been claimed that Fe ions have a formal 3+ oxidation state with $3d^5$ electronic configuration, while Mo ions are in 5+ state with $4d^1$ electronic configuration. It is well-known that the most stable oxidation state of Mo is 6+ ($4d^0$) and one rarely encounters 5+ oxidation state of Mo in molybdenum compounds. Earlier neutron diffraction studies⁸ have reported the absence of any appreciable moment at the Mo sites, suggesting a $\text{Mo}^{6+}\text{-Fe}^{2+}$ configuration^{8,9}. Fe^{57} Mössbauer results have been interpreted¹⁰ as indicative of an oxidation state of Fe less than 3+. However, several neutron diffraction and Mössbauer reports have also been interpreted as providing evidence for formal $\text{Fe}^{3+}\text{-Mo}^{5+}$ configuration^{11,12}. Since the analysis of neutron and Mössbauer data are model-dependent, it is obviously necessary to obtain much more direct informations concerning the electronic and magnetic properties of this compound. The most unusual observation concerning this compound is the relatively high magnetic transition temperature, though the magnetic Fe ions are far separated by other normally nonmagnetic ions, Mo and O. In such a situation, one would expect a weakly antiferromagnetic system, as indeed found in the case of the analogous compound, Sr_2FeWO_6 , with a Néel temperature, $T_N \sim 37$ K^{7,13}. In contrast, $\text{Sr}_2\text{FeMoO}_6$ is a ferromagnet with $T_C \sim 415$ K^{3,4}. It is to be noted that there are several other examples of both ferromagnetic and antiferromagnetic compounds within the $\text{A}_2\text{BB}'\text{O}_6$, double perovskite oxide series; for example, $\text{Sr}_2\text{CrMoO}_6$ and $\text{Sr}_2\text{FeReO}_6$ are ferromagnetic, while Sr_2FeWO_6 , $\text{Sr}_2\text{MnMoO}_6$ and $\text{Sr}_2\text{CoMoO}_6$ are antiferromagnetic¹⁴⁻¹⁷. Thus, an explanation of the magnetic structure of $\text{Sr}_2\text{FeMoO}_6$ must also be consistent with such diverse properties observed within the same double perovskite family.

2. Crystal structure and magnetoresistive properties of $\text{Sr}_2\text{FeMoO}_6$

2.1 Crystal structure and band structure calculation results

The crystal structure of $\text{Sr}_2\text{FeMoO}_6$ is similar to that of an ordered perovskite structure where Fe^{3+} and Mo^{5+} ions have alternate occupancies at the B sites of the perovskite ABO_3 structure. We show the structure in figure 1 where the arrows represent the crystallographic axes (a , b , c). The compound has a tetragonal unit cell with cell dimensions $a = b = 5.57$ Å, and $c = 7.9$ Å and a space group of $I4/mmm$. Extensive band structure results from several groups^{3,18} have suggested that the ordering between Fe^{3+} and Mo^{5+} ions leads to a half-metallic ferromagnetic (HMFM) state, where only minority spins are present at the Fermi level. We show results of a typical calculation¹⁸ of the density of states (DOS) along with the partial Fe d , Mo d and O p DOS in figure 2. The spin integrated DOS and partial DOS are shown in figure 2a, while the corresponding spin-up and spin-down components are shown in figures 2b and c respectively. It can be easily seen from figure 2b that there is a substantial gap in the spin-up DOS across the Fermi energy, E_F , while the spin-down channel shows finite and continuous DOS across the E_F in agreement with the metallic state of the system. The most important consequence of this is that the mobile charge carriers in this system are fully spin-polarized. The effect of Fe/Mo mis-site disorder has also been investigated by similar *ab-initio* band structure calculations¹⁸. The effect of disorder was simulated within supercell calculations to realize several configurations

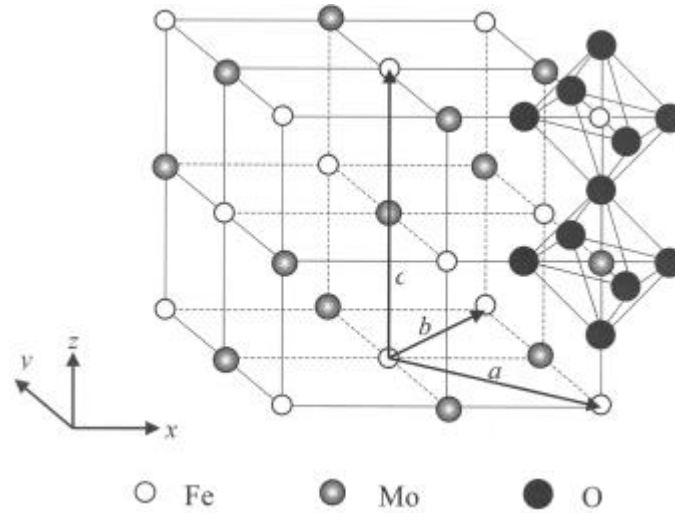


Figure 1. Schematic structure of $\text{Sr}_2\text{FeMoO}_6$. Sr atoms are not shown and only a few oxygen atoms are shown for clarity. The cubic axes (x, y, z) as well as the crystallographic axes (a, b, c) are shown in the figure (adapted from ref. 6).

with mis-site disorders. It is found that such disorder effects destroy the half-metallic ferromagnetic state of the ordered compound, leading to decrease of the magnetic moment.

2.2 Effect of Fe/Mo mis-site disorder on magnetoresistance

We have synthesized highly ordered ($\sim 90\%$) and extensively disordered ($\sim 30\%$) polycrystalline $\text{Sr}_2\text{FeMoO}_6$ samples¹². In figure 3, we show the percentage magnetoresistance, % MR, defined as,

$$\% \text{ MR}(T, H) = 100 \times [\mathbf{r}(T, H) - \mathbf{r}(T, 0)] / \mathbf{r}(T, 0),$$

where $\mathbf{r}(T, H)$ is the resistivity of the sample at a temperature, T and in presence of an applied magnetic field strength H , for the ordered and the disordered samples at 4.2 K. The ordered sample is characterized by sharp and pronounced magnetoresistive responses (30% MR) in the low field regime (< 1 tesla). This low field response is most probably contributed by the spin scattering across different magnetic domains in these polycrystalline samples and this response depends on the presence of the HFMF state arising from the high degree of Fe/Mo ordering. The absence of low-field magnetoresistance (LFMR) response in our disordered sample (figure 3) clearly establishes the fact that high degree of disordering destroys the HFMF state and consequently the LFMR response and this LFMR response has a linear dependence with the Fe/Mo antisite disorder, present in this series of samples¹⁹. It is to be noted that the presence of high ordering, and so the HFMF state, alone cannot ensure a high LFMR response, because this low field response comes from the spin-polarized charge

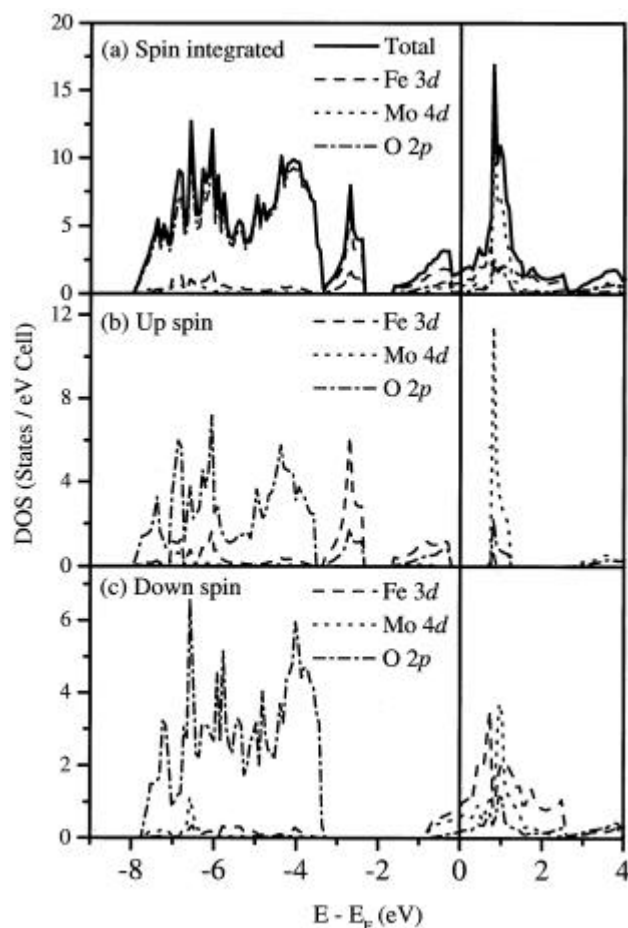


Figure 2. Total density of states (DOS) along with partial Fe d , Mo d and O p DOS are shown in the panels (adapted from ref. 6). (a) Shows the spin-integrated densities, while (b) and (c) show the same for up- and down-spin channels respectively.

carrier scattering at the grain boundaries and so grain boundaries also have an important role to play in determining this effect. This suggestion is supported by the absence of sharp LFMR effect in highly ordered single crystalline bulk²⁰ and epitaxial thin film²¹ samples of $\text{Sr}_2\text{FeMoO}_6$.

3. Formal oxidation states of Fe and Mo in $\text{Sr}_2\text{FeMoO}_6$

We have already mentioned in §1 that the formal oxidation state of Fe in $\text{Sr}_2\text{FeMoO}_6$ is still a matter of controversy. It was suggested earlier that Fe is in the formal 3+ state^{3,12}, while many recent reports claim that the oxidation state of Fe is actually much less than 3+, e.g. 2.5+ or even 2+^{8,10}. Some of these conclusions are based on the analysis of Fe^{57} Mössbauer data, while some of them come from the results of neutron diffraction experiments, where no moment was found on Mo. All these arguments

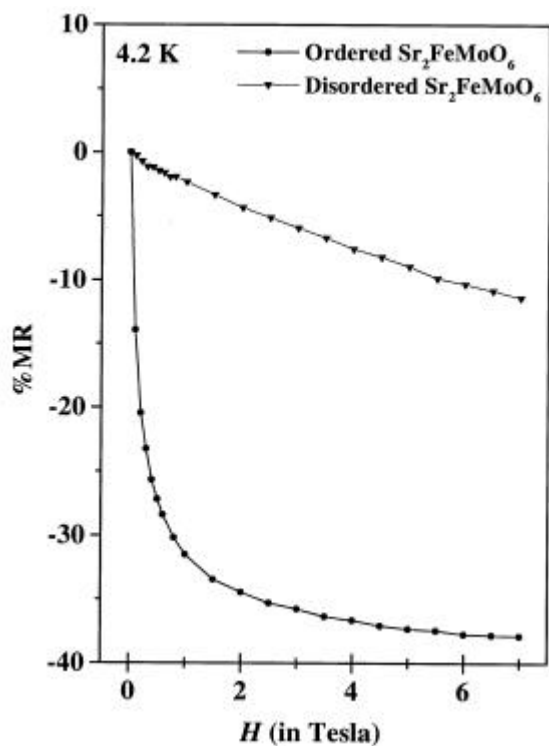


Figure 3. %MR of ordered and disordered $\text{Sr}_2\text{FeMoO}_6$ samples as a function of applied magnetic field (H) at 4.2 K (adapted from ref. 12).

suggest that the minority d band of Fe is also occupied, which can in fact be seen in all band structure results (figure 2). The occupancy of the minority d -state occurs via covalent mixing of these states with other states, such as the O $2p$ and Mo $4d$ states, due to the presence of large hopping interaction strengths. Such covalent mixing is well-known in every transition metal oxide systems, such as LaFeO_3 ²². However, this does not necessarily imply that Fe, either in LaFeO_3 or in $\text{Sr}_2\text{FeMoO}_6$, has fractional valency. The question of formal valency is related⁶ to the question of which ionic configuration provides a better starting point for describing the ground state of the system within a configuration interaction approach.

3.1 X-ray absorption (XAS) results

In order to probe the valence state of Fe experimentally, it is most suitable to investigate the Fe $2p_{3/2}$ XAS which exhibits very clear differences between formal Fe^{2+} and Fe^{3+} states²³. The XAS spectrum of Fe $2p_{3/2}$ edge in $\text{Sr}_2\text{FeMoO}_6$ is shown in figure 4. From this figure it is evident, even in the absence of any detailed analysis, that only a Fe^{3+} valence state is consistent with the experimental spectrum, exhibiting a weaker lower energy shoulder and a higher energy main peak, which is a characteristic feature of trivalent Fe compounds²³. The divalent Fe state exhibits a reversed intensity pattern with the weaker intensity shoulder appearing at the higher energy side of the main peak. In order to provide a quantitative description of the spectral features,

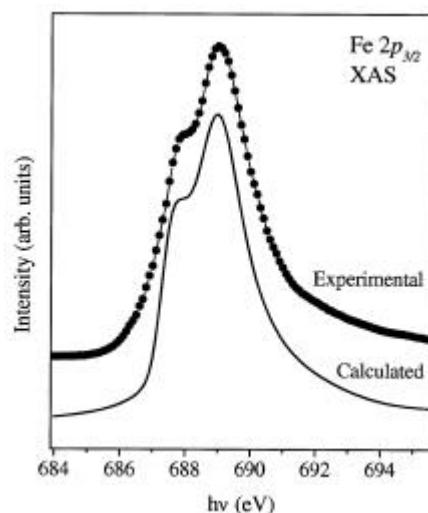


Figure 4. Experimental and calculated Fe $2p_{3/2}$ X-ray absorption spectra for ordered $\text{Sr}_2\text{FeMoO}_6$ (adapted from ref. 24).

detailed calculations were carried out²⁴ to simulate the experimental spectrum within a cluster model, including hybridization effects with the ligands on an equal footing with core–valence and valence–valence multiplet interactions and crystal field effects²⁵. This calculation yields a remarkably good description of the experimental spectrum, as shown in figure 4. The many-body ground state has 60.2% d^5 , 34.5% $d^6\bar{L}^1$ and 5.1% $d^7\bar{L}^2$ character, suggesting the system to be somewhat more ionic than even LaFeO_3 ²². It should be noted here that it was not possible to describe the spectral features starting with a formal Fe^{2+} configuration.

3.2 X-ray magnetic circular dichroism (XMCD) study

Recently, site specific X-ray magnetic circular dichroism (XMCD) experiments have been performed on $\text{Sr}_2\text{FeMoO}_6$ to probe site-specific magnetic moments at the Fe and the Mo sites²⁴. In figures 5a and b we show the results of XAS experiments with circularly polarized light at the Fe $2p \rightarrow 3d$, and Mo $3p \rightarrow 4d$ edges respectively. The XMCD spectra, also shown in corresponding panels clearly show a large magnetic moment on Fe. It is evident from the XMCD spectrum of Mo that there is no detectable moment on Mo, in agreement with a previous neutron diffraction measurement⁸. This result establishes that the spin-density of the single, itinerant electron in the minority spin channel, responsible for the metallic behaviour of the compound, is not substantially at the Mo site. This is also in agreement with the expectation based on band structure results that this single electron is extensively delocalized over Fe and O sites along with the Mo site.

4. Magnetic structure of $\text{Sr}_2\text{FeMoO}_6$

It had been suggested earlier^{3,7,12} that this compound has alternate occupancies of nominal $\text{Mo}^{5+} 4d^1 S=1/2$ and $\text{Fe}^{3+} 3d^5 S=5/2$ ions along three cubic axes. The

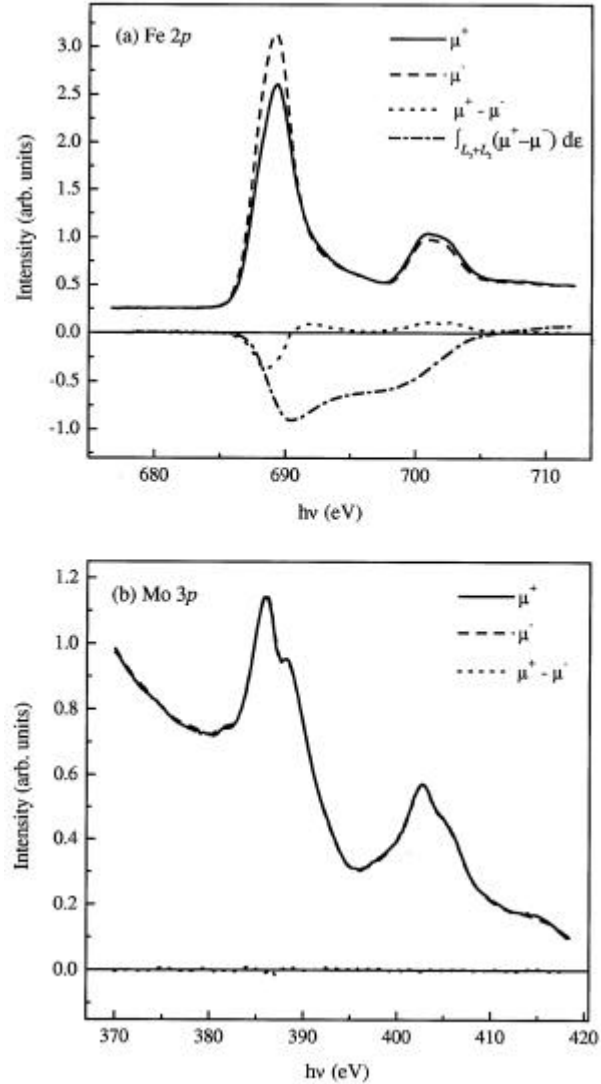


Figure 5. X-ray absorption spectra at (a) Fe 2p and (b) Mo 3p edges for ordered $\text{Sr}_2\text{FeMoO}_6$, measured using circularly polarized light. In the lower part of each figure the dichroic signals for the corresponding edges are shown. The integral difference spectrum for the Fe 2p edge is also shown in the lower part of (a) (adapted from ref. 24).

individual Fe and Mo sublattices are coupled ferromagnetically while the two sublattices are antiferromagnetically coupled to each other to give rise to a $S=2$ per formula unit. It has been often implicitly assumed²⁶ that an antiferromagnetic superexchange is responsible for the coupling between the Fe and Mo sites and, consequently, the driving force for the observed magnetic structure. This appears to be improbable, since a superexchange type coupling between the Fe d states to the highly

delocalized Mo d states will at best be weak, and therefore, incompatible with the unusually high ordering temperature in this compound. If superexchange interaction were to be dominant in the system, it would definitely suggest that any 180° Fe–O–Fe bond, if present, will be antiferromagnetically coupled. Recently, a detailed *ab-initio* band structure calculations have been carried out¹⁸, using supercells to simulate mis-site disorder between Fe and Mo sites and thereby creating several such Fe–O–Fe interactions in the system. Significantly, this calculation shows that all Fe ions are ferromagnetically coupled irrespective of Fe–O–Fe bonds in the system. This suggests that the system, instead of being considered as an antiferromagnetically coupled Fe and Mo sublattices, should be viewed as a system with ferromagnetically coupled Fe ions, mediated via an antiferromagnetic coupling to the delocalized electron.

In close analogy to the case of manganites, it has been suggested at times^{8,27} that a double exchange mechanism⁵ is responsible for the ferromagnetic coupling between the Fe sites. In case of manganites, the spin moment of t_{2g} localized states couple ferromagnetically to the spin of e_g delocalized electron, due to intra-atomic Hund's coupling strength, I , arising from the exchange stabilization of the parallel spin arrangement. For $\text{Sr}_2\text{FeMoO}_6$, the same mechanism cannot be invoked because of the antiparallel alignment of localized and delocalized spins, making the I between the parallelly oriented localized and delocalized electrons, which provides the energy scale of the on-site spin coupling in the double exchange mechanism for the manganites, irrelevant⁶.

4.1 A new mechanism of magnetic interaction

A novel kinetic energy driven mechanism has recently been proposed²⁸ to explain the magnetic interaction between the localized and the conduction electrons, leading to ferromagnetic coupling of the Fe ions. The proposed mechanism is shown as a schematic diagram in figure 6. The Fe $3d$ levels are shown at the left side of the figure

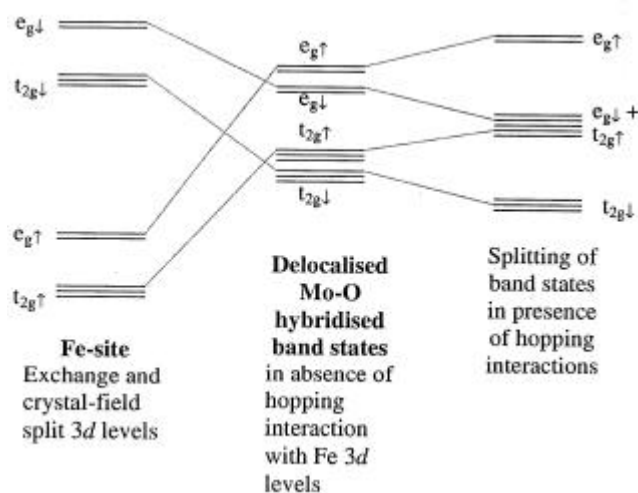


Figure 6. Schematic of various energy level diagrams to explain the origin of the proposed magnetic interaction in $\text{Sr}_2\text{FeMoO}_6$ and related compounds (adapted from ref. 28).

with a relatively small crystal field splitting compared to the large exchange splitting of the d levels as expected for $\text{Fe}^{3+} 3d^5$ systems^{28,29}. Delocalized Mo–O hybridized states appear at higher energies compared to the occupied Fe d states and have higher crystal field and lower exchange splitting in the absence of any hopping interaction. These states are shown in the central panel of figure 6. In the presence of hopping interactions, there is strong coupling between the Fe states and the delocalized states, leading to perturbations to these bare energy levels. Hybridization with the corresponding Fe states pushes the delocalized $t_{2g\uparrow}$ states up and $t_{2g\downarrow}$ further down in energy due to bonding–antibonding splitting. This is shown in the right part of figure 6. The shifts of up and down spin states in the opposite directions lead to a large effective exchange splitting, and consequently to a pronounced spin-polarization of the conduction band; the system is stabilized by populating the down spin band and, therefore, ensuring antiferromagnetic coupling between the localized Fe and the itinerant electron. Detailed many-body calculations²⁸ suggest that this antiferromagnetic coupling strength in $\text{Sr}_2\text{FeMoO}_6$ is about 18 meV, which explains the presence of such high magnetic T_c in this compound.

5. Evidence of high correlation in $\text{Sr}_2\text{FeMoO}_6$

While much of the discussion in this article is motivated by results based on effectively single-particle band theories, there is strong evidence that details of the electronic and magnetic structures of $\text{Sr}_2\text{FeMoO}_6$ cannot be entirely described by such approaches due to the presence of pronounced correlation effects. We have already pointed out that the analysis of X-ray absorption spectral features (figure 4) within a many-body approach indicates that the system is more correlated than LaFeO_3 . Moreover, the estimate of the antiferromagnetic coupling strength between the localized Fe majority spin and the minority spin conduction band is properly estimated only by such many-body approaches, emphasizing the importance of correlation effects in the system.

5.1 High resolution valence band photoemission results

The most evident manifestation of correlation effects, arising from the substantial intraatomic Coulomb interaction strength within the Fe $3d$ manifold, is found in the valence band photoemission spectrum of this material³⁰, shown in figure 7. For comparison, we also show the calculated DOS for ordered $\text{Sr}_2\text{FeMoO}_6$, obtained by band structure calculation over the relevant energy range in the same figure. From this comparison, it is evident that experimentally obtained spectral features are not accurately described by the effectively single-particle band structure calculations performed within the local spin-density approximation. Most significantly, the remarkably intense feature at about 8.1 eV binding energy in the experimental spectrum lies below the bottom of the calculated band, shown by the vertical dashed line. Thus, it is clear that this feature is the correlation driven satellite feature, similar to the ones observed in the case of other strongly correlated systems, such as NiO ³¹ and U-intermetallics³². We note that this satellite is intense for $\text{Sr}_2\text{FeMoO}_6$ and is undoubtedly the highest among all Fe^{3+} oxides studied so far³³. This unusually strong correlation can be qualitatively understood in terms of the crystal structure of this compound. In ordered $\text{Sr}_2\text{FeMoO}_6$, the effective Fe–Fe hopping interaction responsible for the bandwidth is significantly weakened due to the large separation between two Fe

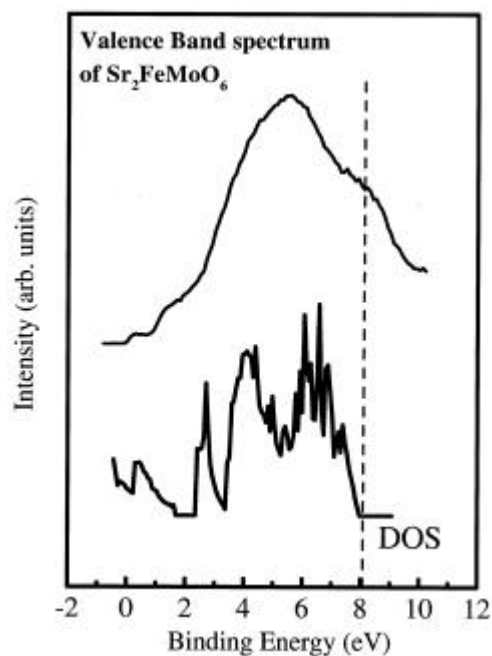


Figure 7. Experimental valence band spectrum of ordered $\text{Sr}_2\text{FeMoO}_6$ is shown along with the DOS, calculated by *ab-initio* band structure method (adapted from ref. 30).

sites by Fe–O–Mo–O–Fe connectivities in all the three directions. This strong reduction of the Fe *d* bandwidth compared to other Fe oxide systems effectively enhances the correlation effect significantly and, thereby, gives rise to the intense satellite feature at 8.1 eV.

6. Summary

In conclusion, we have discussed the electronic and magnetic properties of $\text{Sr}_2\text{FeMoO}_6$, defining a new class of magnetic materials, exhibiting interesting CMR properties with possible technological relevance. We have shown that this class of compounds should be considered as a system of ferromagnetically coupled localized spins, mediated via a pronounced antiferromagnetic coupling of the localized spins to the delocalized electrons.

References

1. von Helmholt R, Wecker J, Holzapfel B, Schultz L and Samwer K 1993 *Phys. Rev. Lett.* **71** 2331; for a review: 1995 (April) *Phys. Today* Special issue on Magnetoelectronics
2. Millis A J, Littlewood P B and Shraiman B I 1995 *Phys. Rev. Lett.* **74** 5144; Millis A J, Littlewood P B and Shraiman B I 1996 *Phys. Rev. Lett.* **77** 175; Millis A J 1998 *Phys. Rev. Lett.* **80** 4358
3. Kobayashi K-I, Kimura T, Sawada H, Terakura K and Tokura Y 1998 *Nature (London)* **395** 677

4. Patterson F K, Moeller W C and Ward R 1963 *Inorg. Chem.* **2** 196; Galasso F S 1966 *J. Chem. Phys.* **44** 1672
5. Zener C 1951 *Phys. Rev.* **B82** 403; Anderson P W and Hasegawa H 1955 *Phys. Rev.* **B100** 67
6. Sarma D D 2001 *Curr. Opin. Solid State Mater. Sci.* **5** 261
7. Nakagawa T, Yoshikawa K and Nomura S 1969 *J. Phys. Soc. Jpn.* **27** 880
8. Garcia L, Ritter C, Ibarra M R, Blasco J, Algarabel P A, Mahendiran R and Garcia J 1999 *Solid State Commun.* **110** 435
9. Goodenough J B and Dass R I 2000 *Int. J. Mater.* **2** 3
10. Linden J, Yamamoto T, Karppinen T A, Yamauchi H and Pietari T 2000 *Appl. Phys. Lett.* **76** 2925
11. Moritomo Y, Sheng X, Machida A, Akimoto T, Nishibori E, Takata M, Sakata M and Ohoyama K 2000 *J. Phys. Soc. Jpn.* **69** 1723
12. Sarma D D, Sampathkumaran E V, Ray S, Nagarajan R, Majumdar S, Kumar A, Nalini G and Guru Row T N 2000 *Solid State Commun.* **114** 465
13. Kawanaka H, Ease I, Toyama S and Nishihara Y 2000 *Physica* **B281-282** 518
14. Arulraj A, Ramesha K, Gopalakrishnan J and Rao C N R 2000 *J. Solid State Chem.* **155** 233
15. Kobayashi K-I, Kimura T, Tomioka Y, Sawada H, Terakura K and Tokura Y 1999 *Phys. Rev.* **B59** 11159
16. Hamada N and Moritomo Y 2000 *The 3rd Japan-Korea Joint Workshop on First-Principles Electronic Structure Calculations*, p. 56
17. Moritomo Y, Xu S, Machida A, Akimoto T, Nishibori E, Takata M and Sakata M 2000 *Phys. Rev.* **B61** R7827
18. Saha-Dasgupta T and Sarma D D 2001 *Phys. Rev.* **B64** 064408
19. Garcia-Hernandez M, Martinez J L, Martinez-Lope M J, Casais M T and Alonso J A 2001 *Phys. Rev. Lett.* **86** 2443
20. Tomioka Y, Okuda T, Okimoto Y, Kumai R, Kobayashi K-I and Tokura Y 2000 *Phys. Rev.* **B61** 422
21. Westerburg W, Reisinger D and Jakob G 2000 *Phys. Rev.* **B62** R767; Yin H Q, Zhou J-S, Zhou J-P, Dass R, McDevitt J T and Goodenough J B 1999 *Appl. Phys. Lett.* **75** 2812; Yin H Q, Zhou J-S, Dass R, Zhou J-P, McDevitt J T and Goodenough J B 2000 *J. Appl. Phys.* **87** 6761
22. Chainani A, Mathew M and Sarma D D 1993 *Phys. Rev.* **B48** 14818
23. van der Laan G and Kirkman I W 1992 *J. Phys.: Condens. Matter* **4** 4189
24. Ray S, Kumar A, Sarma D D, Cimino R, Turchini S, Zennaro S, Zema N 2001 *Phys. Rev. Lett.* **87** 097204
25. Mahadevan P and Sarma D D 2000 *Phys. Rev.* **B61** 7402
26. Ogale A S, Ramesh R and Venkatesan T 1999 *Appl. Phys. Lett.* **75** 537
27. Kim T H, Uehara M, Cheong S W and Lee S 1999 *Appl. Phys. Lett.* **74** 1737; Martinez B, Navarro J, Balcells L and Fontcuberta J 2000 *J. Phys.: Condens. Matter* **12** 10515
28. Sarma D D, Mahadevan P, Saha-Dasgupta T, Ray S and Kumar A 2000 *Phys. Rev. Lett.* **85** 2549
29. Mahadevan P, Shanthi N and Sarma D D 1997 *J. Phys.: Condens. Matter* **9** 3129
30. Our unpublished results
31. Fujimori A, Minami F and Sugano S 1984 *Phys. Rev.* **B29** 5225
32. Allen J W, Oh S-J, Cox L E, Ellis W P, Wire M S, Fisk Z, Smith J L, Pate B B, Lindau I and Arko A J 1985 *Phys. Rev. Lett.* **54** 2635; Sarma D D, Hillebrecht F U, Speier W, Mrtensson N and Koelling D D 1986 *Phys. Rev. Lett.* **57** 2215
33. Sarma D D, Shanthi N, Barman S R, Hamada N, Sawada H and Terakura K 1995 *Phys. Rev. Lett.* **75** 1126; Sarma D D, Shanthi N and Mahadevan P 1996 *Phys. Rev.* **B54** 1622